LISSOM Orientation Maps

Dr. James A. Bednar

jbednar@inf.ed.ac.uk

http://homepages.inf.ed.ac.uk/jbednar

Modeling Orientation

- Starting point: Retinotopy model
- Same architecture, different input pattern
- Three dimensions of variance: x, y, orientation
- How will that fit into a 2D map?

Retinotopy input and response

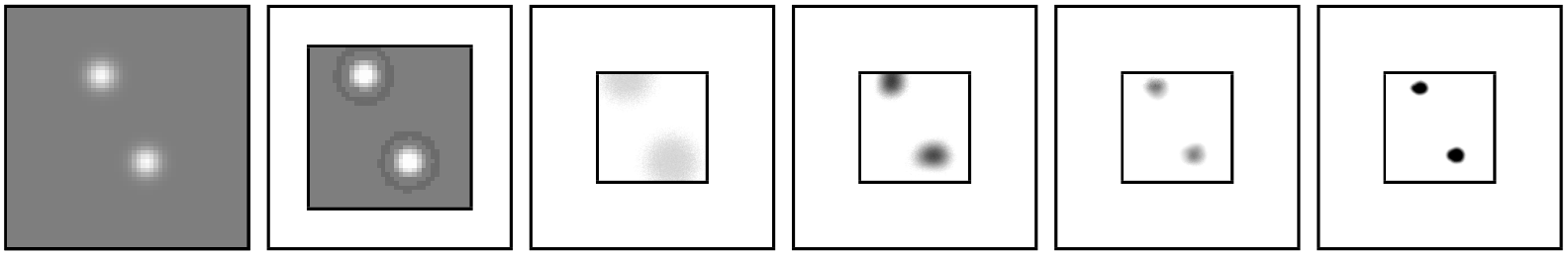

Retinal activation	LGN response	Iteration 0: Initial V1 response	Iteration 0: Settled V1 response	10,000: Initial V1 response	10,000: Settled V1 response

CMVC figure 4.4

(Reminder from last time)

Orientation input and response

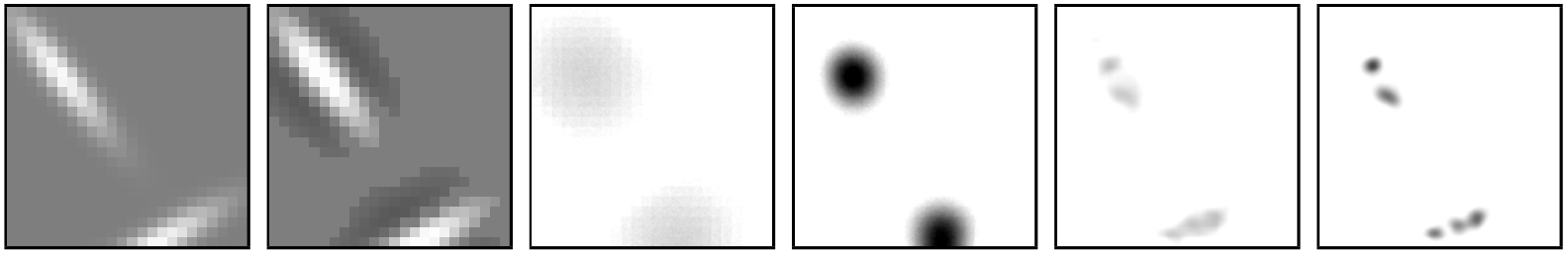

Retinal activation	LGN response	Iteration 0: Initial V1 response	Iteration 0: Settled V1 response	10,000: Initial V1 response	10,000: Settled V1 response

CMVC figure 5.6

- Response before training similar to retinotopy case
- Response after training has multiple activity blobs per input pattern
- Blobs are orientation-specific

Self-organized V1 weights

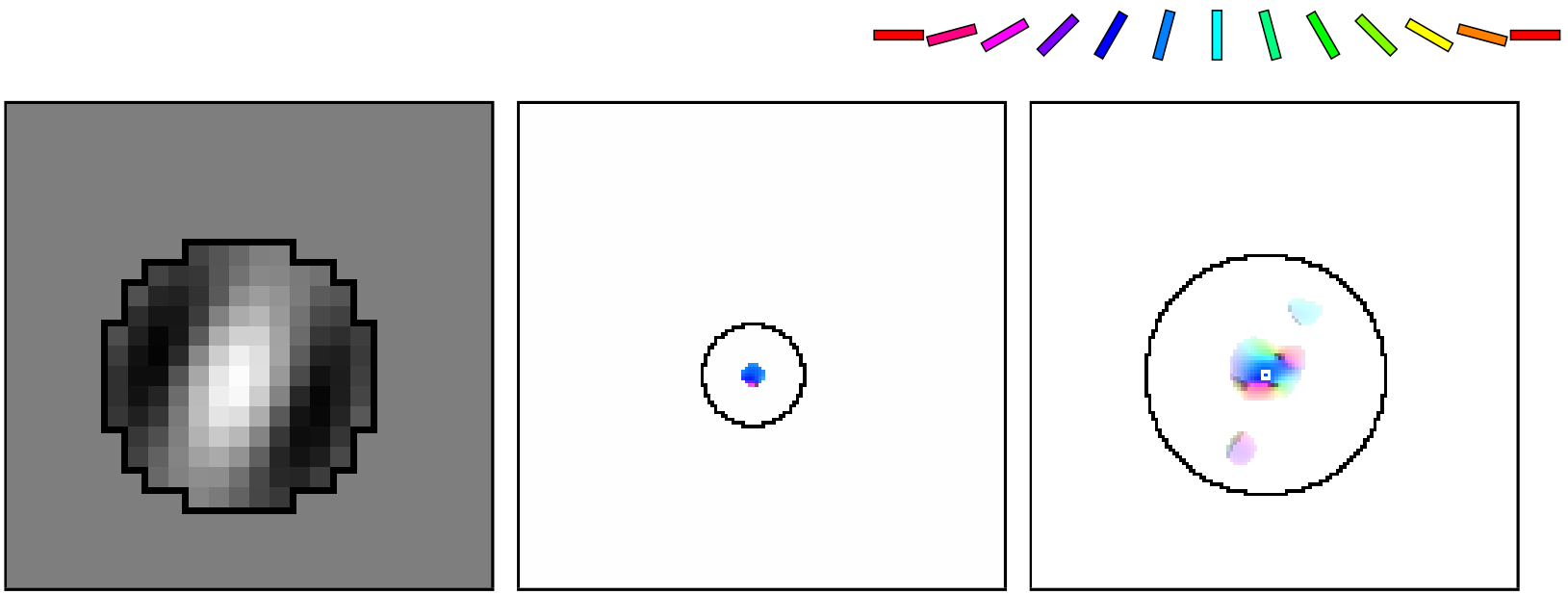

Afferent (ON—OFF) Lateral excitatory Lateral inhibitory

CMVC figure 5.7

Typical:

- Gabor-like afferent CF
- Nearly uniform short-range lateral excitatory
- Patchy, orientation-specific long-range lateral inhibitory

Self-organized weights across V1

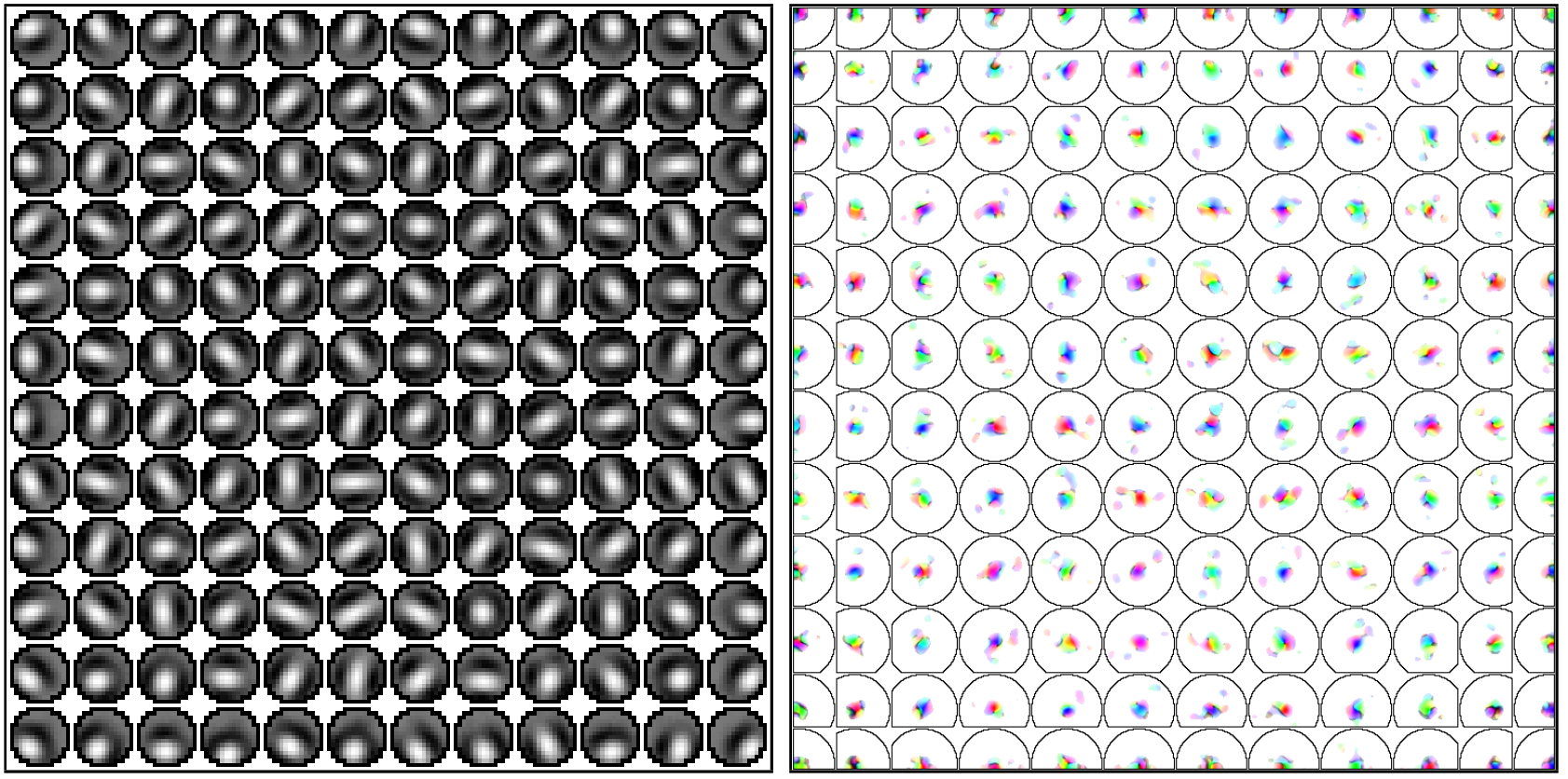

CMVC figure 5.8

Afferent (ON—OFF)

Lateral inhibitory

OR map self-organization

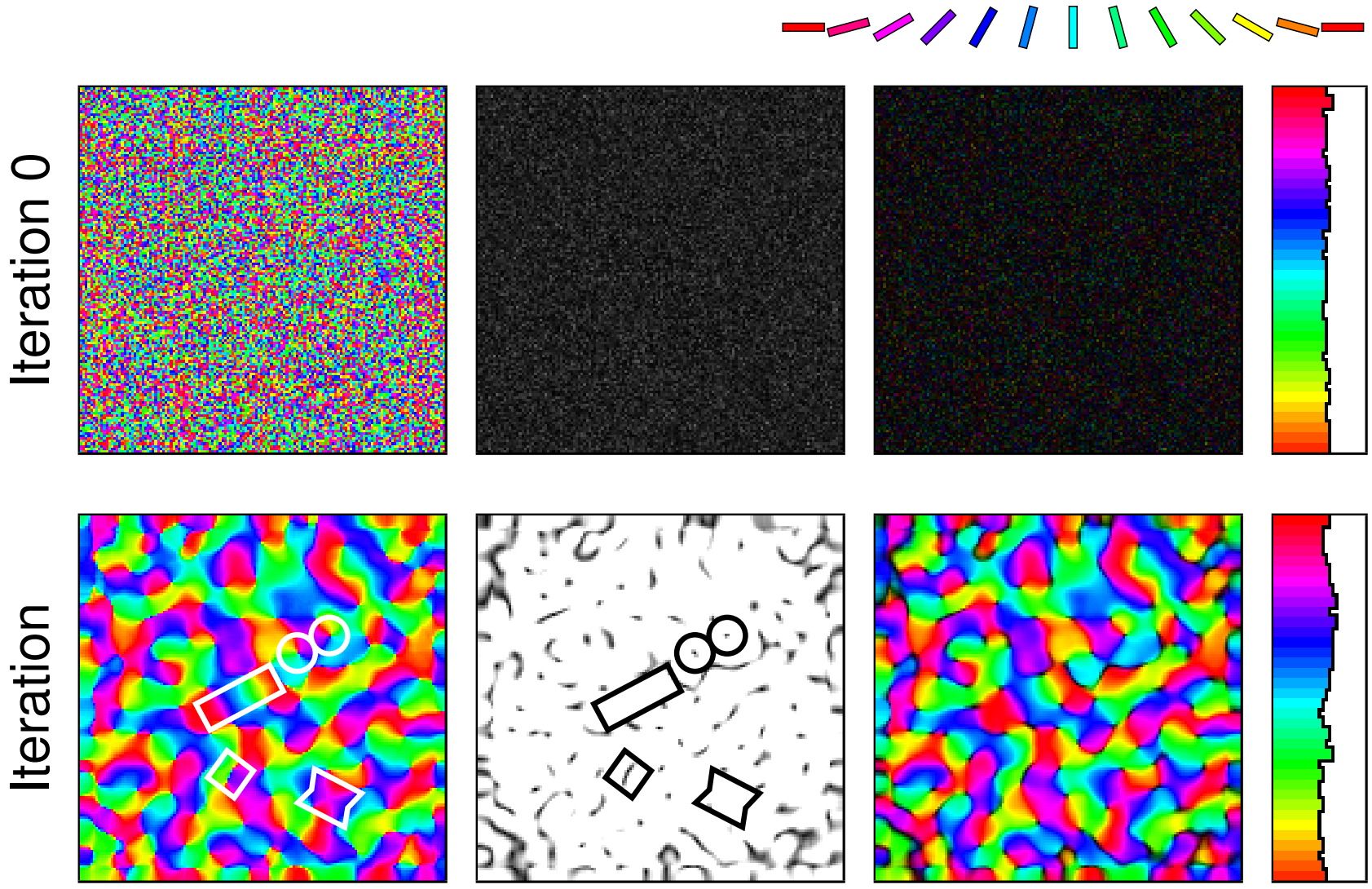

CMVC figure 5.9

Macaque ORmap: Fourier,gradient

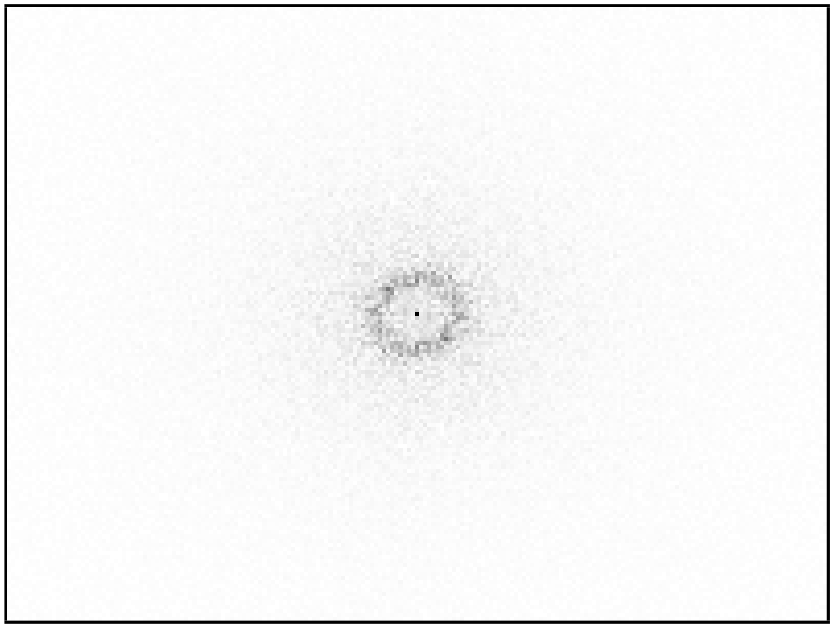

Fourier spectrum

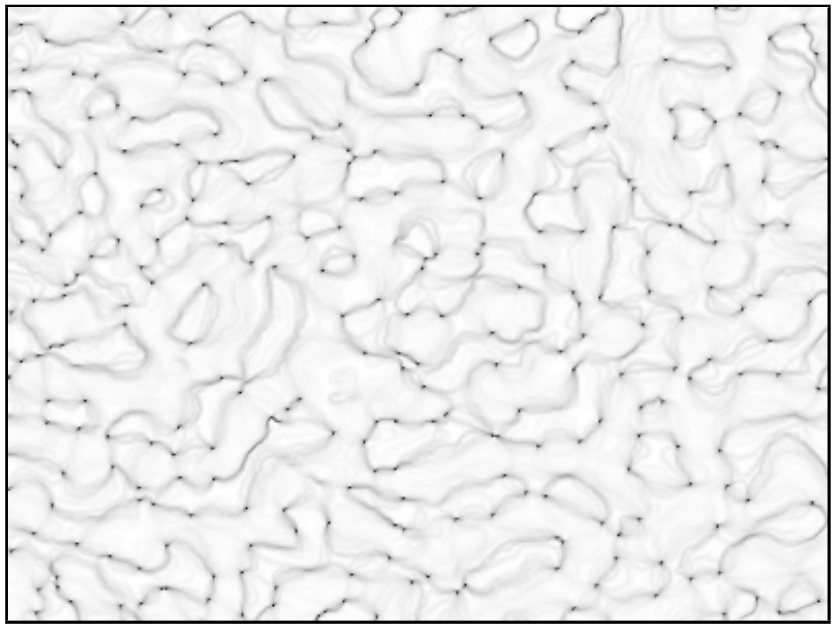

Gradient

CMVC figure 5.1

In monkeys:

- Ring-shaped spectrum:
  repeats regularly in all directions
- High gradient at fractures, pinwheels.

OR Map: Fourier, gradient

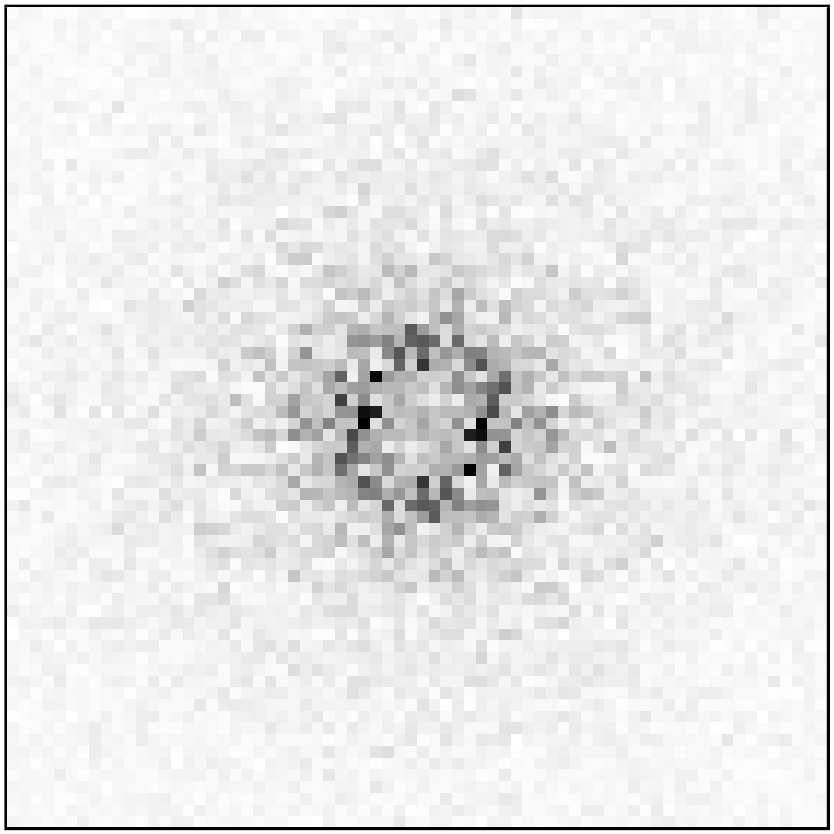

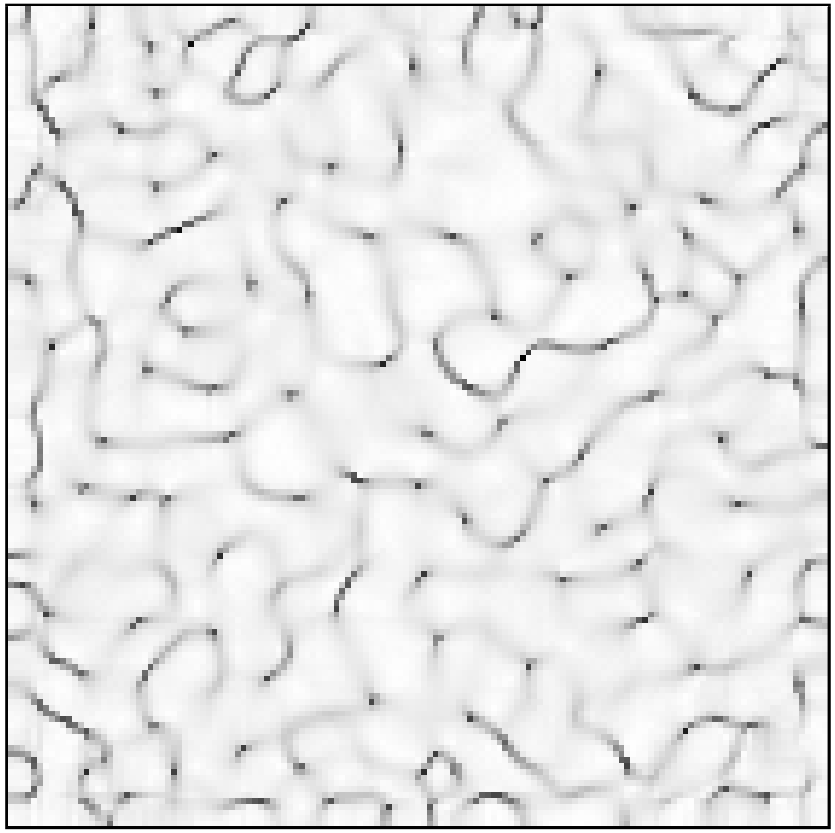

CMVC figure 5.10

Fourier spectrum

Gradient

LISSOM model has similar spectrum, gradient

OR Map: Retinotopic organization

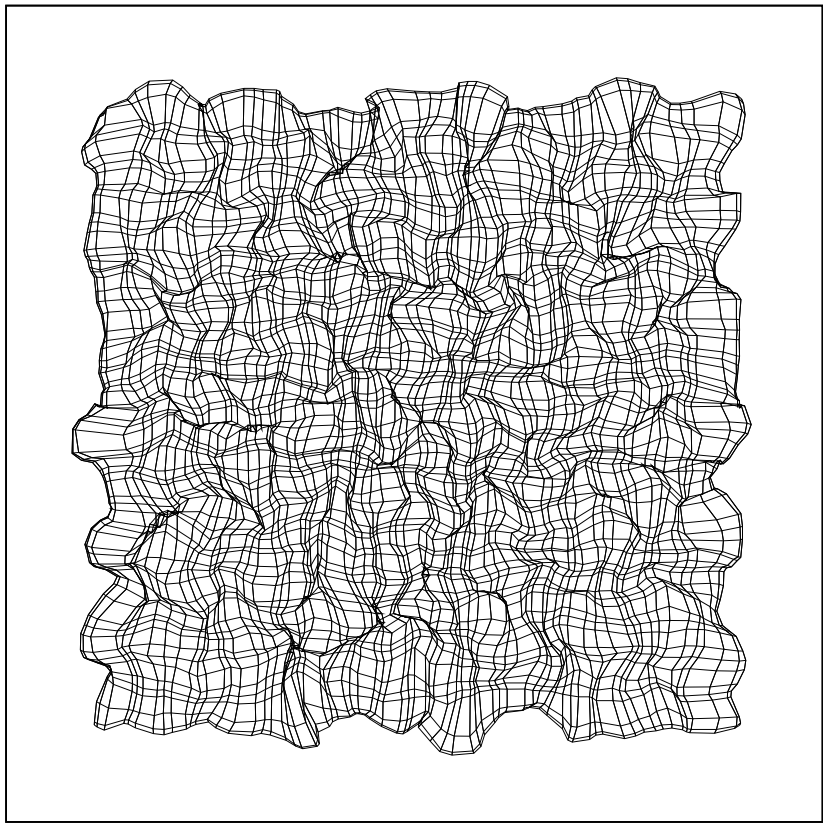

CMVC figure 5.11

- Retinotopy is distorted locally by orientation prefs
- Matches distortions found in animal maps?

OR Map: Lateral connections

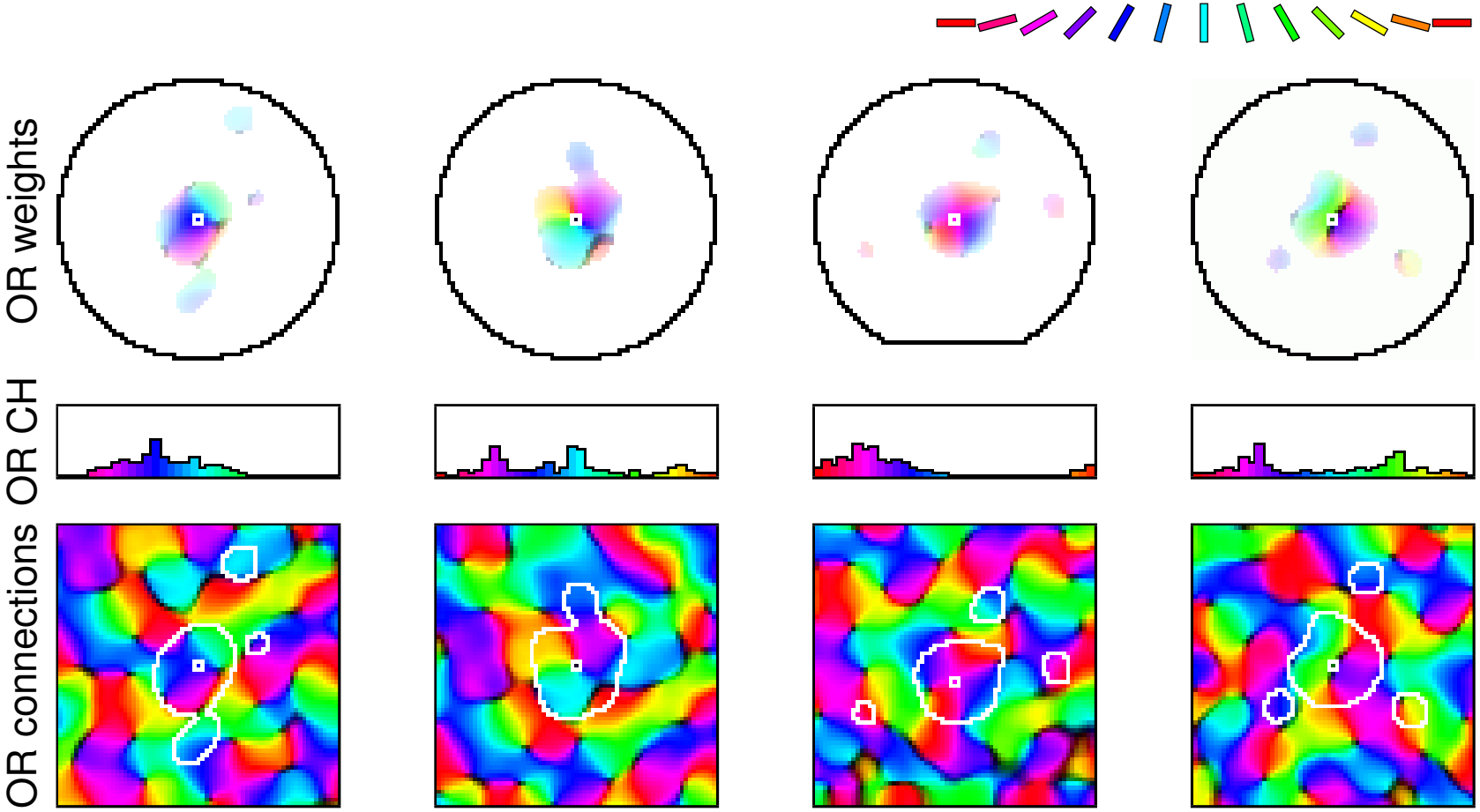

CMVC figure 5.12

Connections in iso-OR patches

Connections in OR pinwheels

Connections in OR saddles

Connections in OR fractures

Effect of initial weights

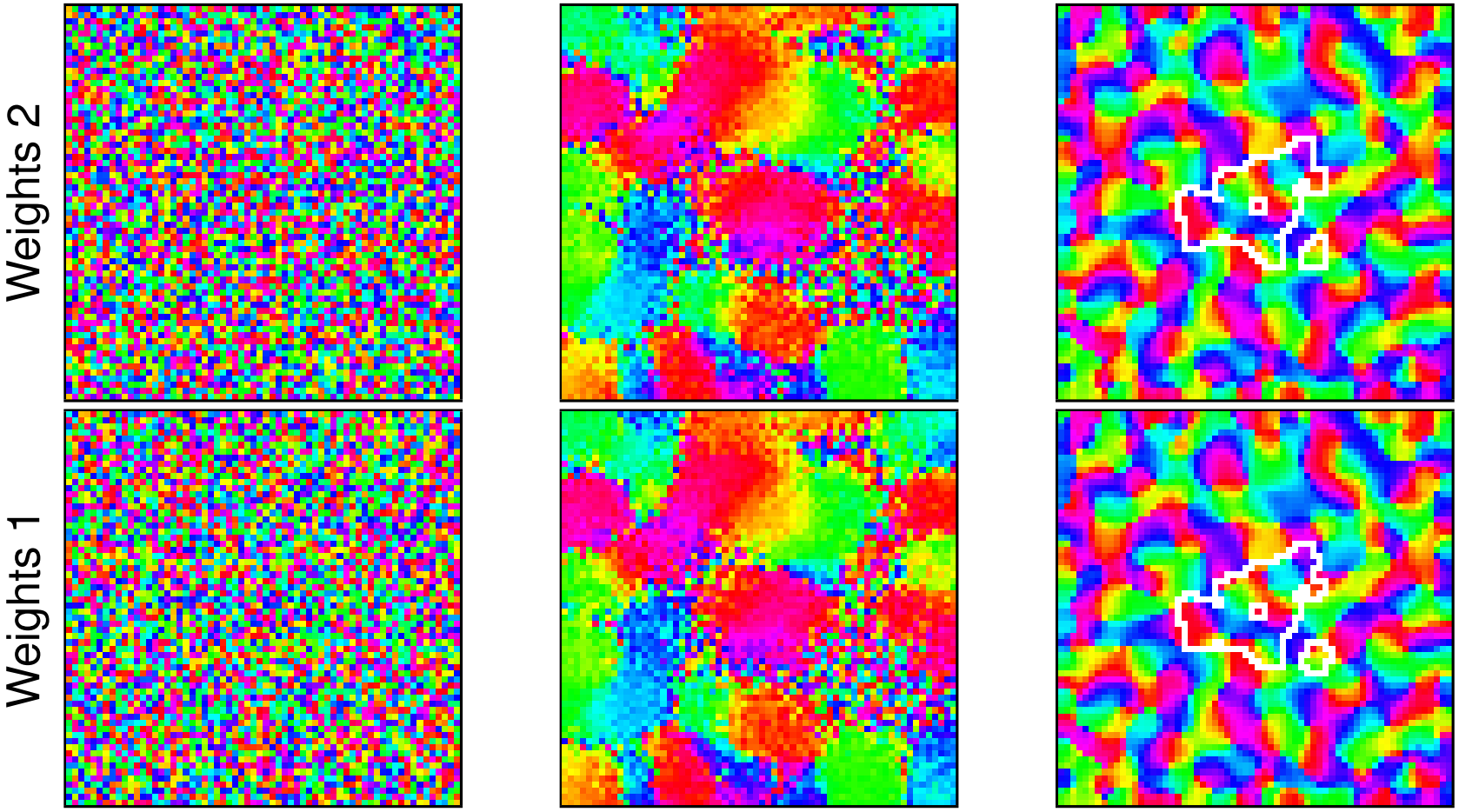

CMVC figure 8.5

(*a*) Iteration 0 (*b*) Iteration 50 (*c*) Iteration 10,000

Changing weights doesn't change map folding pattern.

Effect of input streams

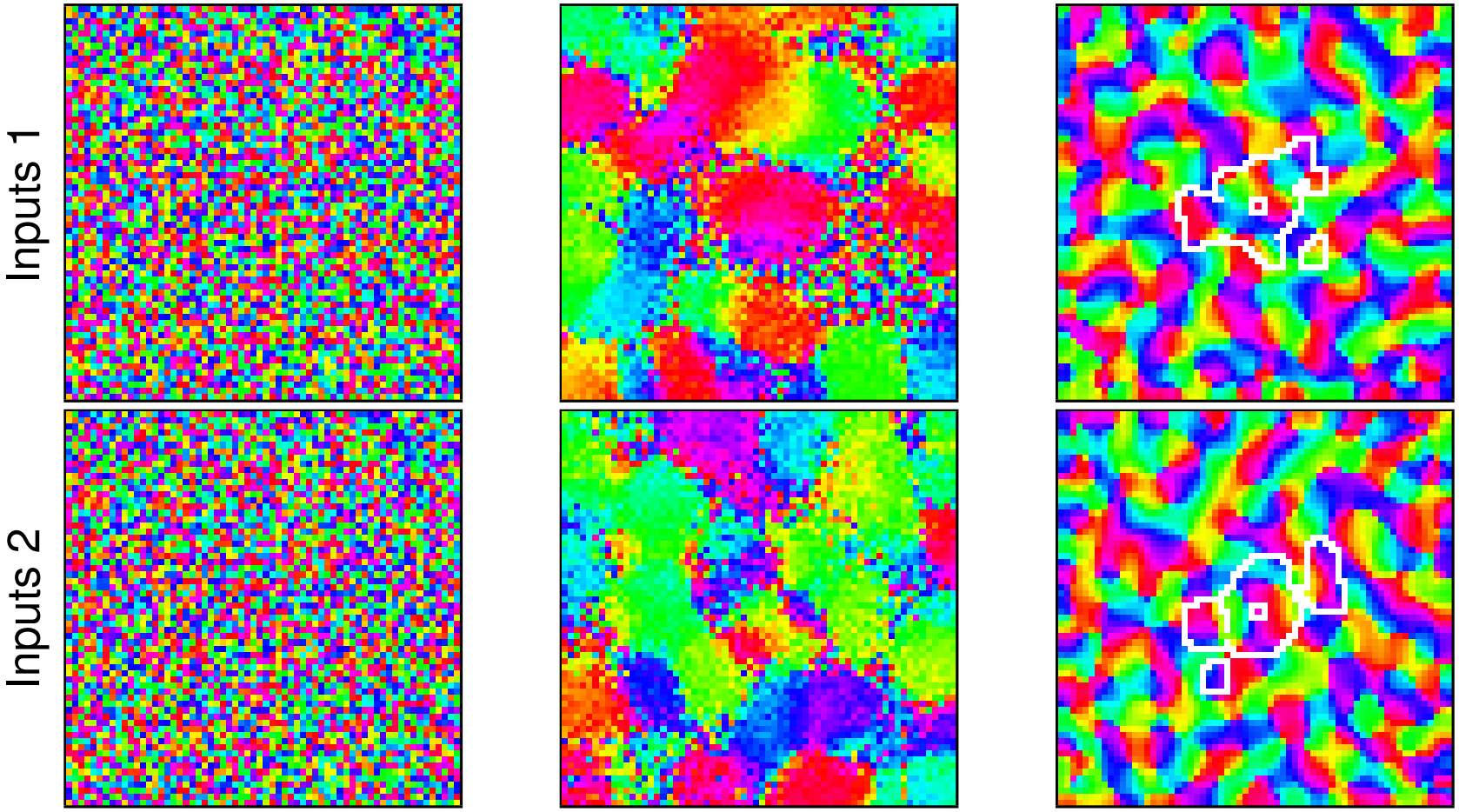

(*a*) Iteration 0 (*b*) Iteration 50 (*c*) Iteration 10,000

CMVC figure 8.5

Changing inputs changes entire pattern.

Scaling retinal and cortical area

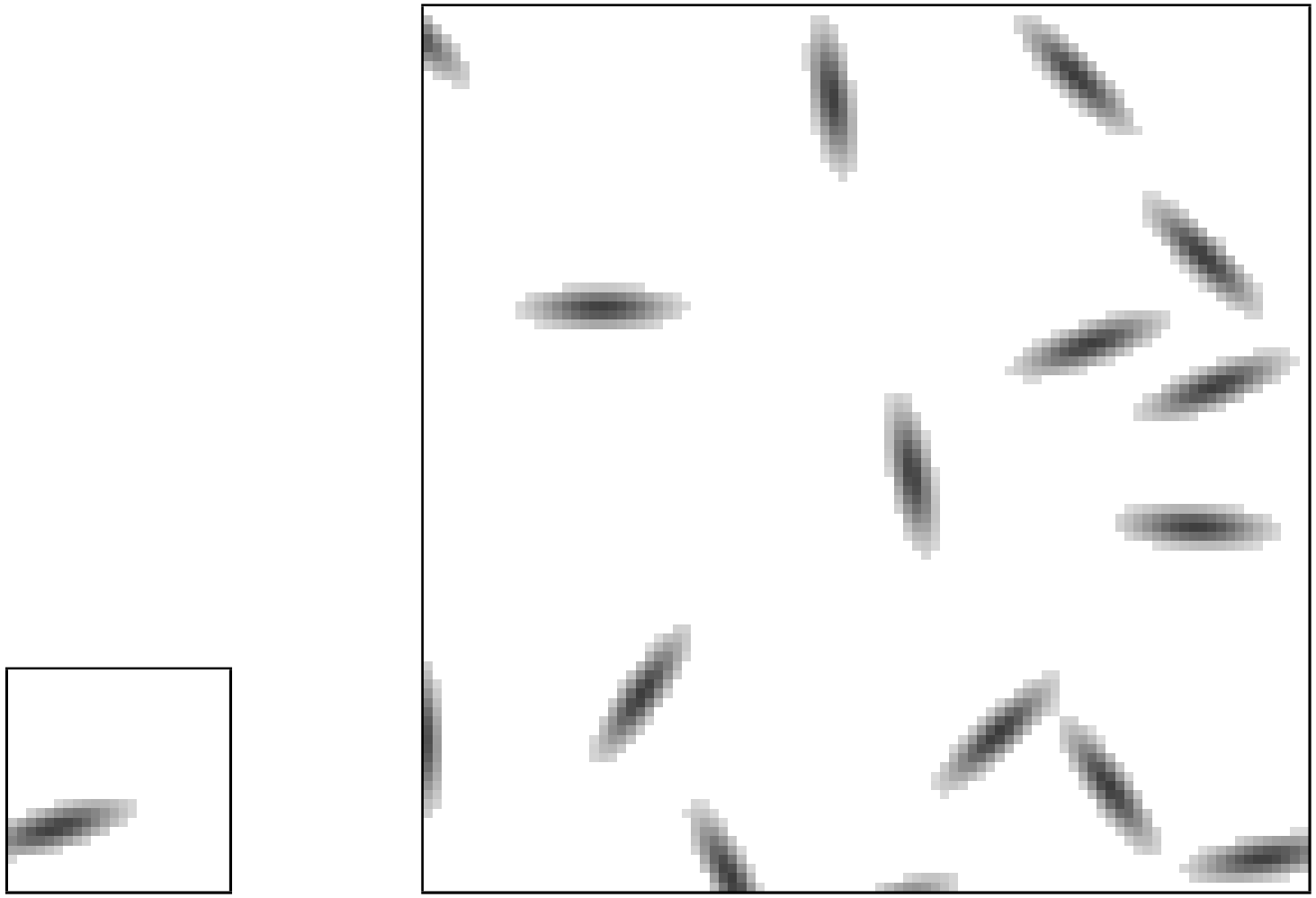

CMVC figure 15.1a,b

(*a*) Original retina: $R = 24$

(*b*) Retinal area scaled by 4.0: $R = 96$

Scaling retinal and cortical area

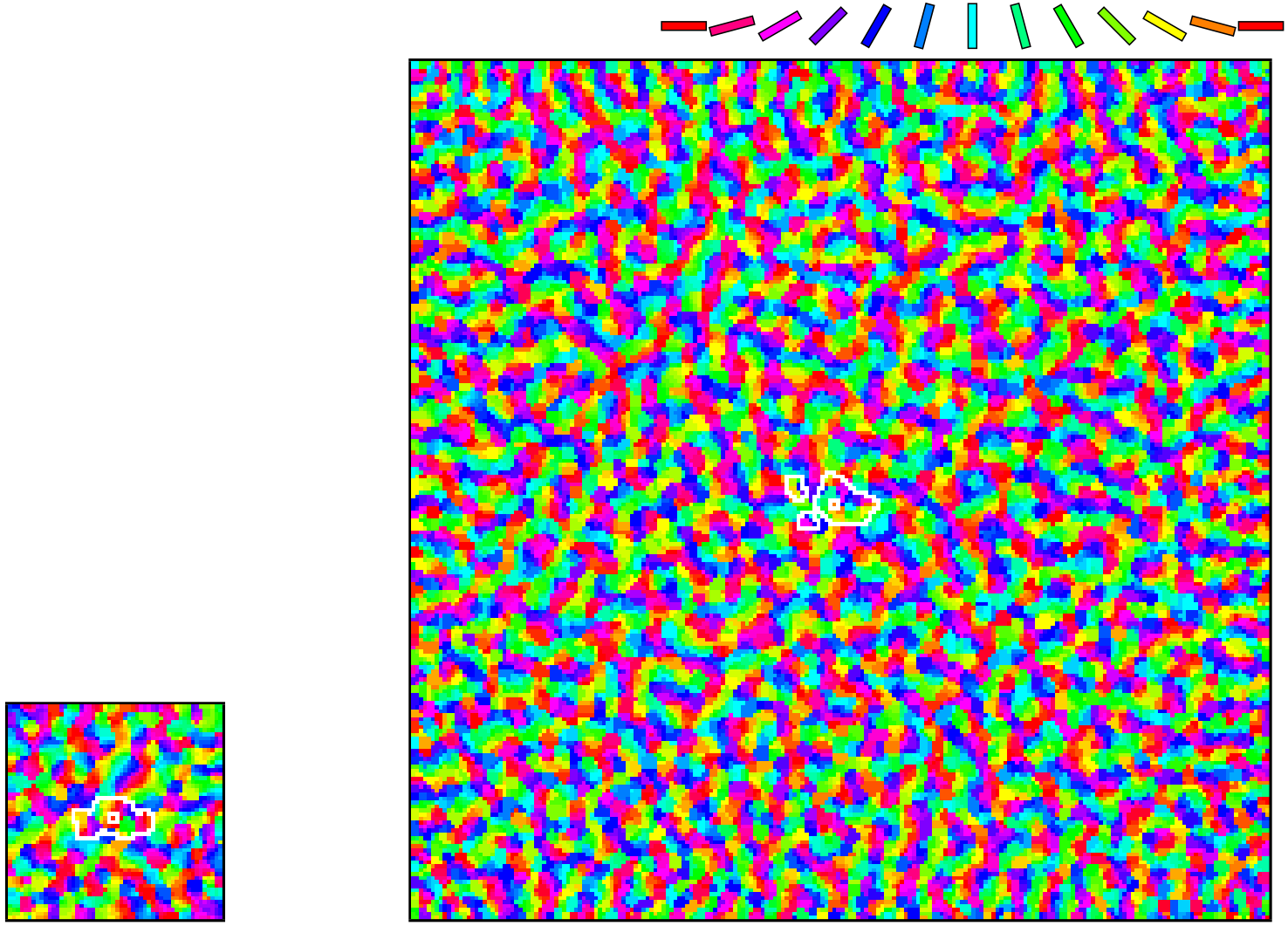

CMVC figure 15.1c,d

(*c*) Original V1:
$N = 54$, 0.4 hours, 8 MB

(*d*) V1 area scaled by 4.0:
$N = 216$, 9 hours, 148 MB

Scaling retinal density

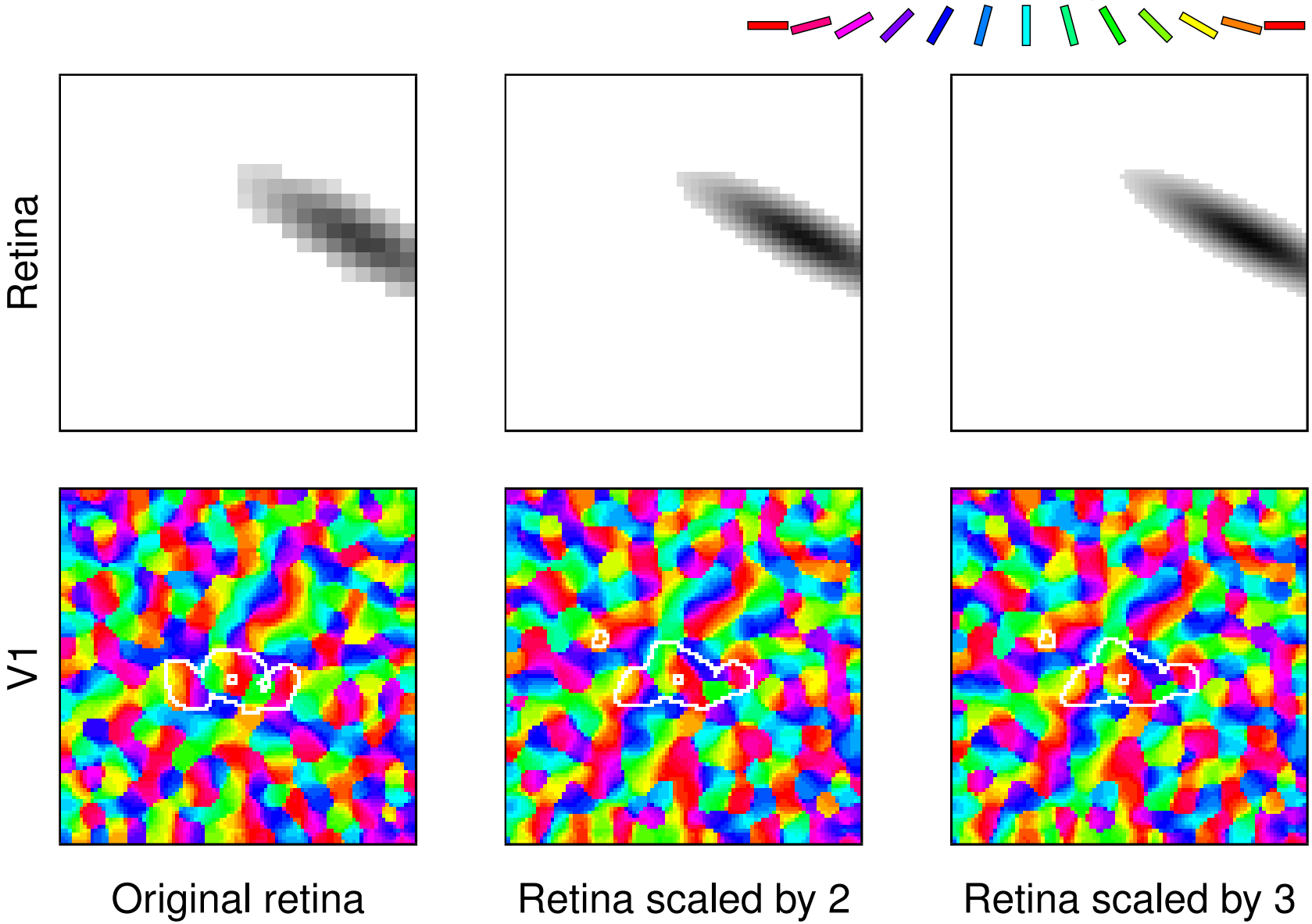

CMVC figure 15.2

Scaling cortical density

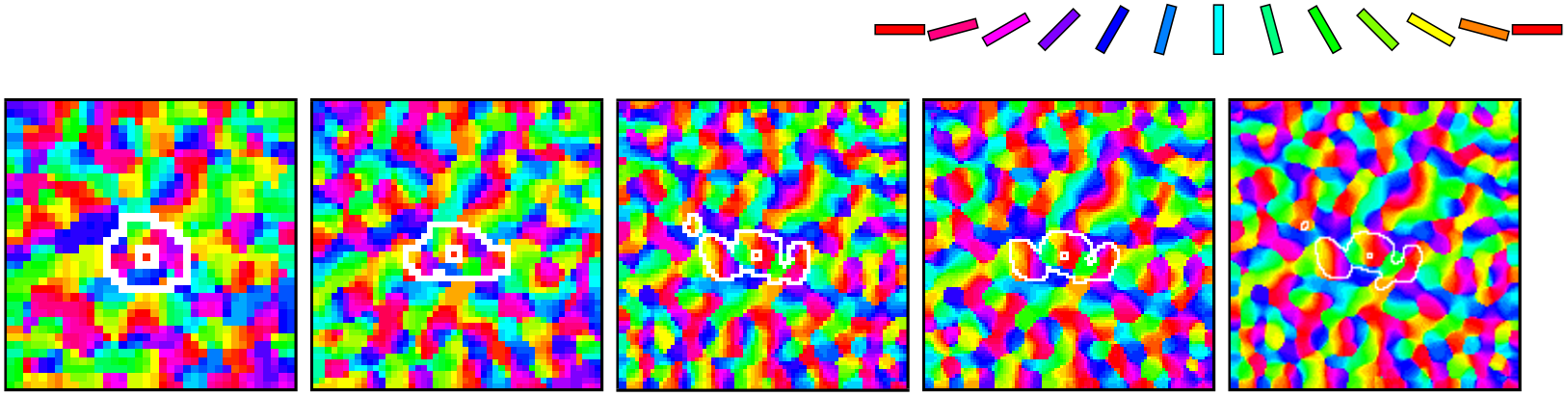

(*a*) 36×36: 0.17 hours, 2.0 MB

(*b*) 48×48: 0.32 hours, 5.2 MB

(*c*) 72×72: 0.77 hours, 22 MB

(*d*) 96×96: 1.73 hours, 65 MB

(*e*) 144×144: 5.13 hours, 317 MB

CMVC figure 15.3

Above minimum density (due to lateral radii),

density not crucial for organization

Full-size V1 Map

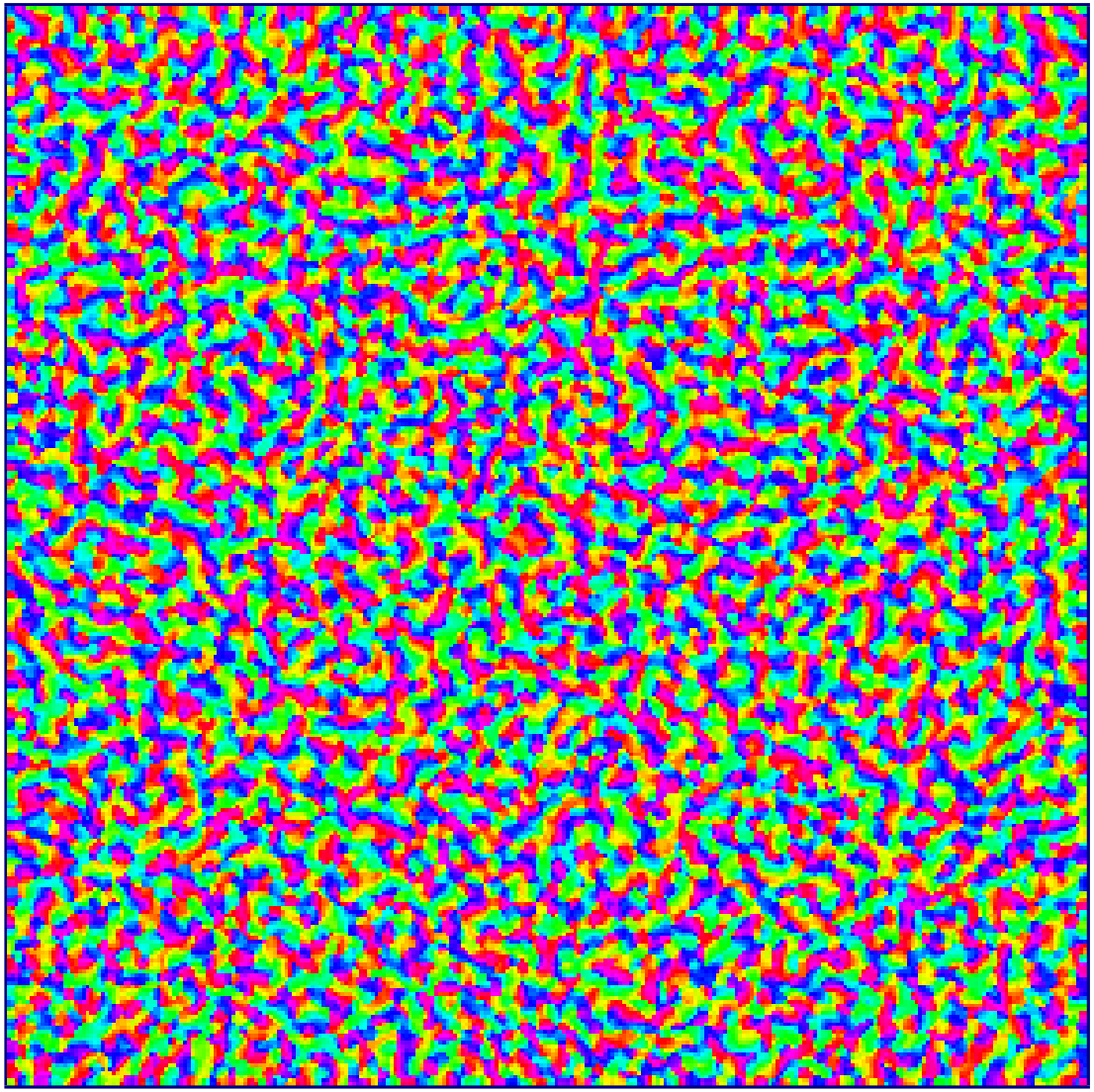

- Map scaled to cover most of visual field
- Allows testing with full-size images
- 30 million connections

Sample Image

RGC/LGN Response

V1 Response with γ_n

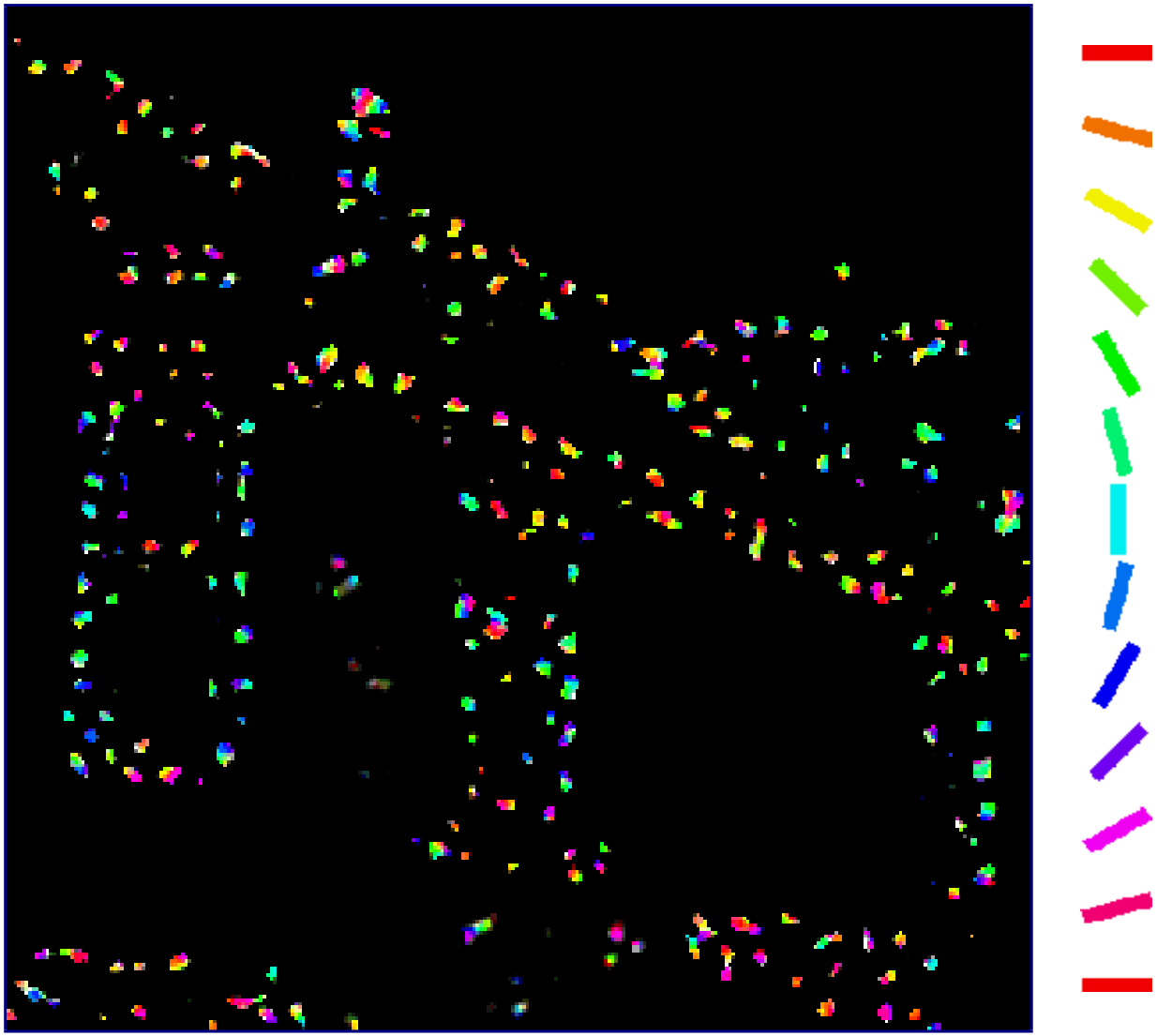

V1 Orientation Map

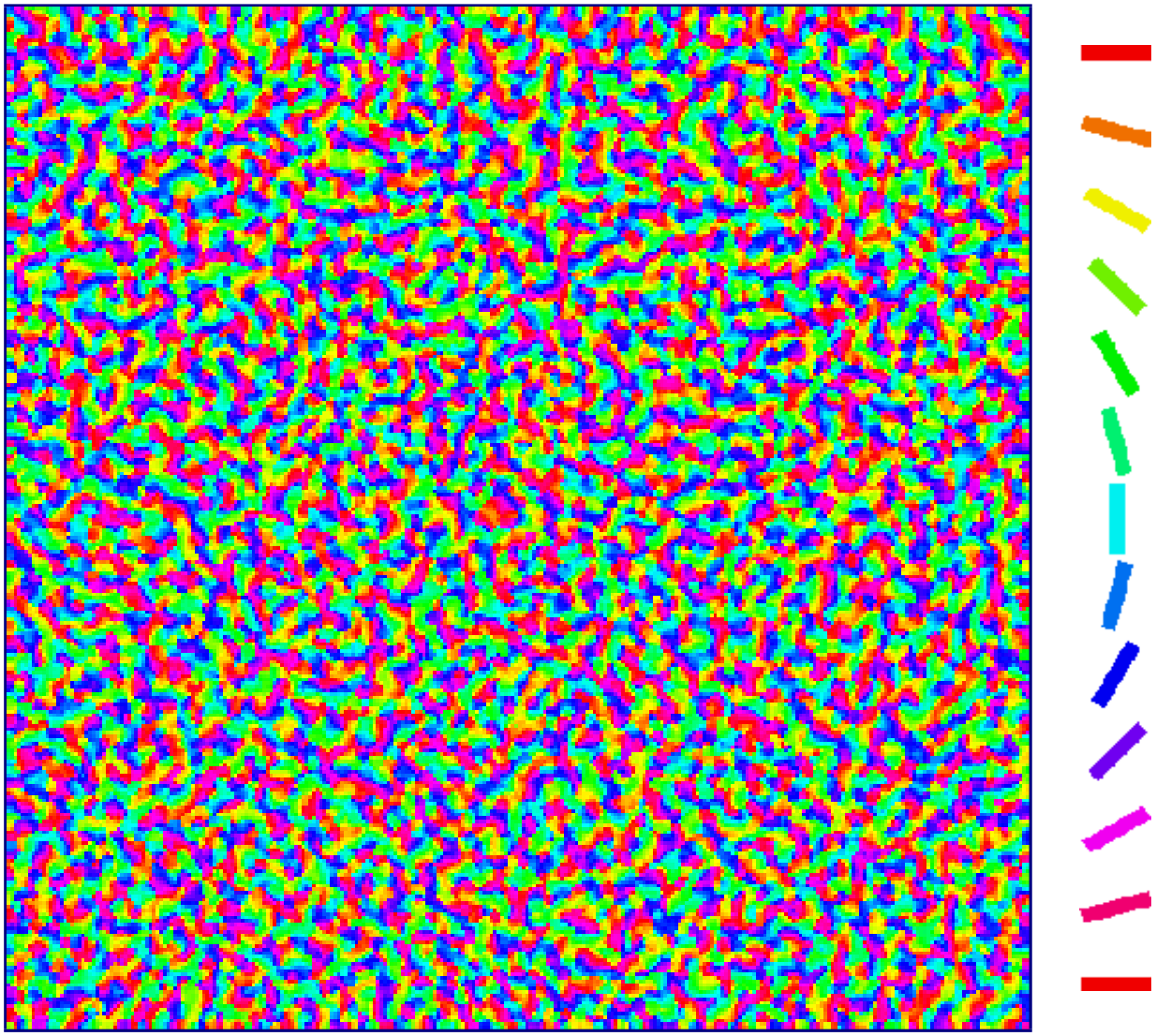

Afferent normalization

Mechanism for contrast invariant tuning:

$$s_{ij} = \frac{\gamma_{\mathrm{A}} \left(\sum_{\rho ab} \xi_{\rho ab} A_{\rho ab,ij} \right)}{1 + \gamma_{\mathrm{n}} \left(\sum_{\rho ab} \xi_{\rho ab} \right)}, \qquad (1)$$

$\xi_{\rho ab}$: activation of unit (a, b) in afferent RF ρ of neuron (i, j)

$A_{ab,ij}$ is the corresponding afferent weight

γ_{A}, γ_{n} are constant scaling factors

RGC/LGN response to large image

CMVC figure 8.2a,b

Retinal activation

LGN response

RGC/LGN responds to most of the visible contours

V1 without afferent normalization

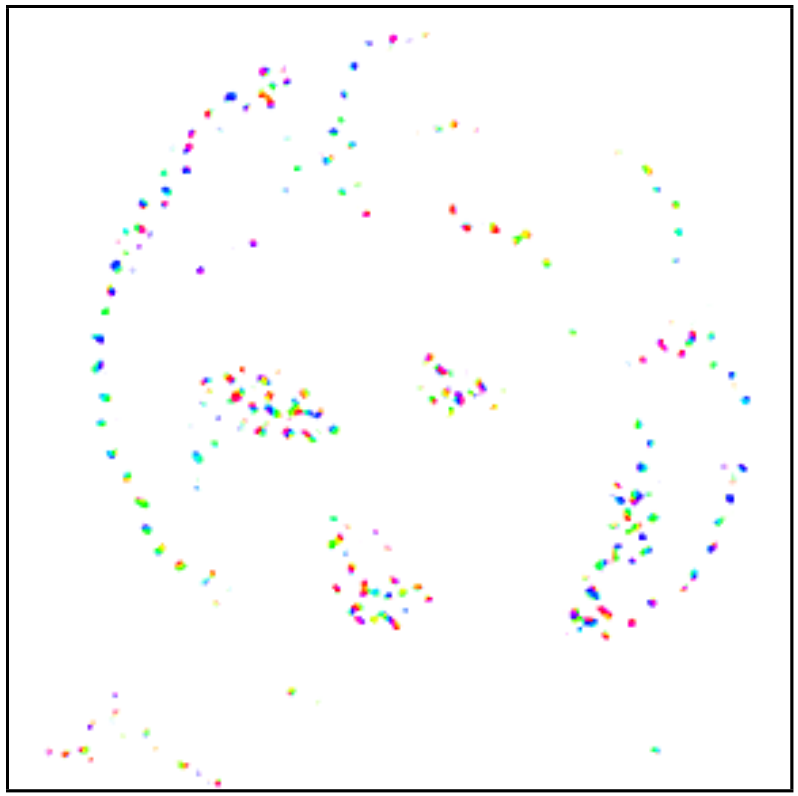

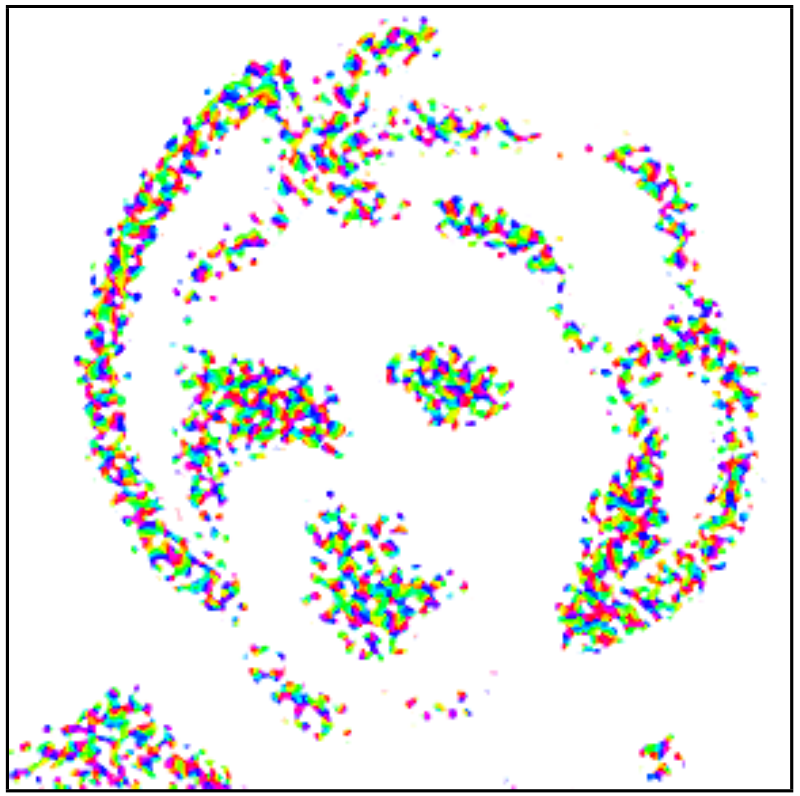

CMVC figure 8.2c-e

V1 response:

$\gamma_{\mathrm{n}} = 0, \gamma_{\mathrm{A}} = 3.25$

V1 response:

$\gamma_{\mathrm{n}} = 0, \gamma_{\mathrm{A}} = 7.5$

Cannot get selective response to all contours

V1 with afferent normalization

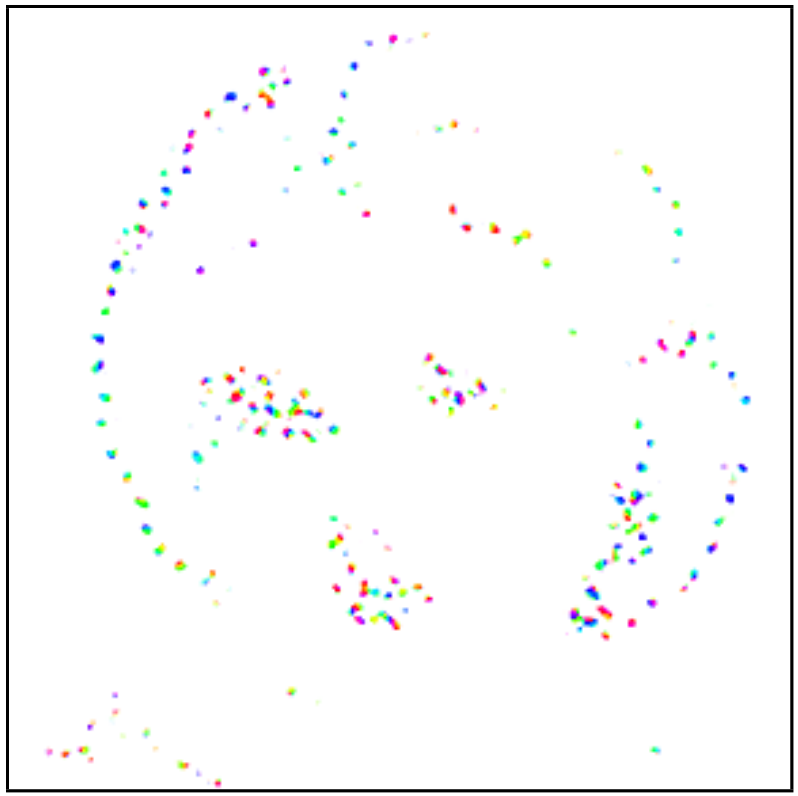

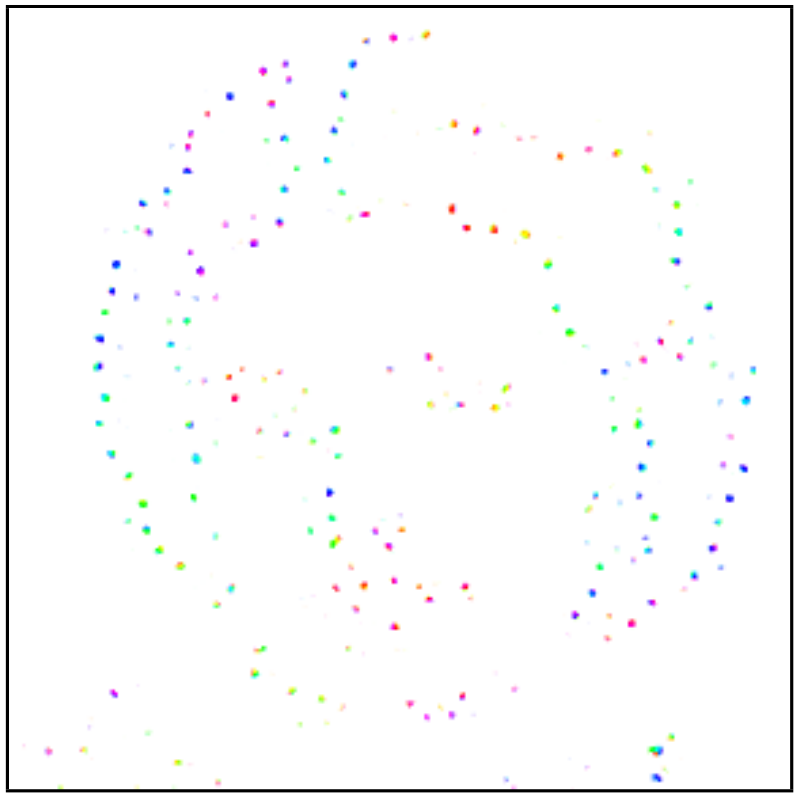

CMVC figure 8.2c-e

V1 response:

$\gamma_{\mathrm{n}} = 0, \gamma_{\mathrm{A}} = 3.25$

V1 response:

$\gamma_{\mathrm{n}} = 80, \gamma_{\mathrm{A}} = 30$

Responds based on contour, not contrast

Tuning with afferent normalization

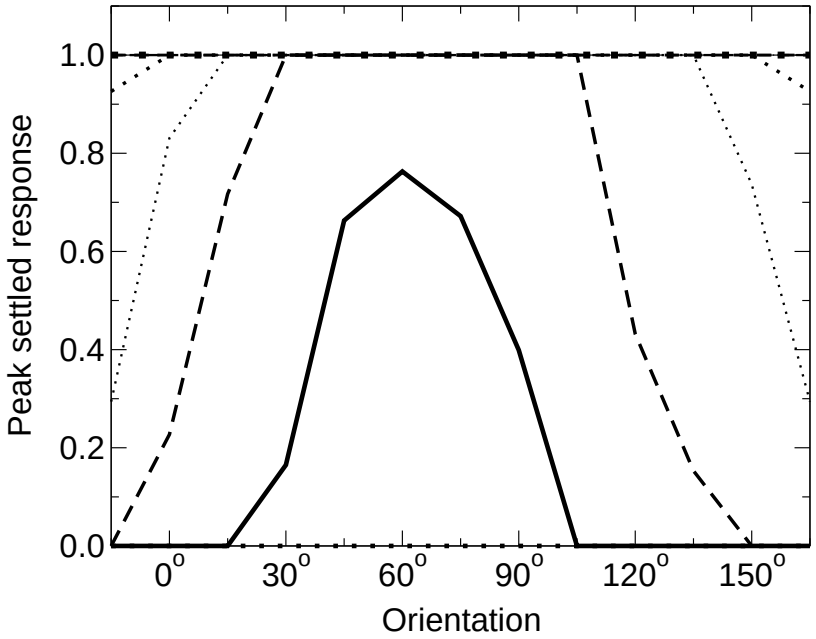

$\gamma_{\mathrm{n}} = 0, \gamma_{\mathrm{A}} = 3.25$

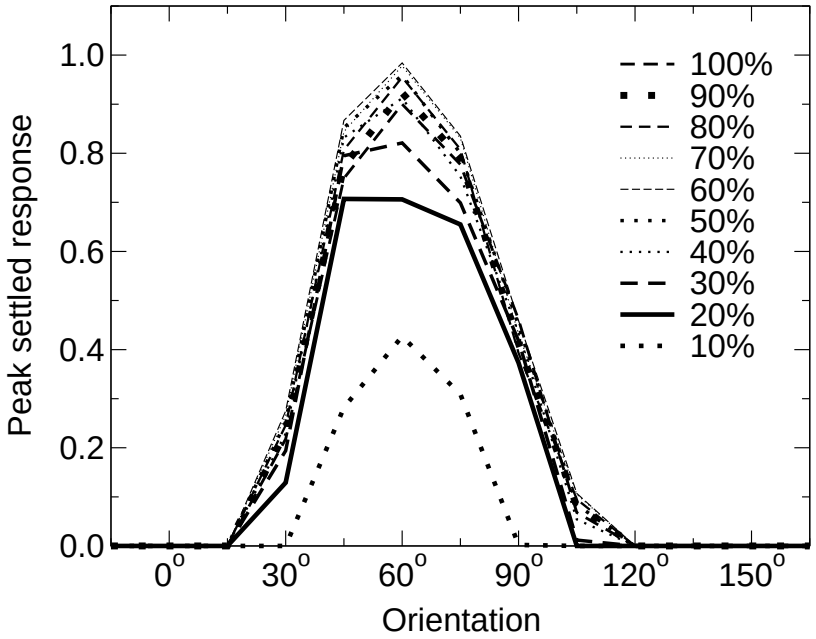

$\gamma_{\mathrm{n}} = 80, \gamma_{\mathrm{A}} = 30$

CMVC figure 8.3

Sine grating tuning curve:

- Without γ_{n}: selectivity lost as contrast increases
- With γ_{n}: always orientation-specific

OR Map: Gaussian

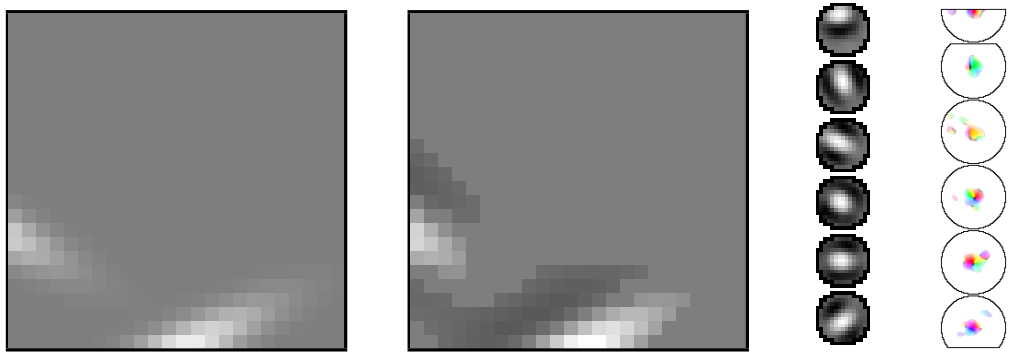

White line RFs only

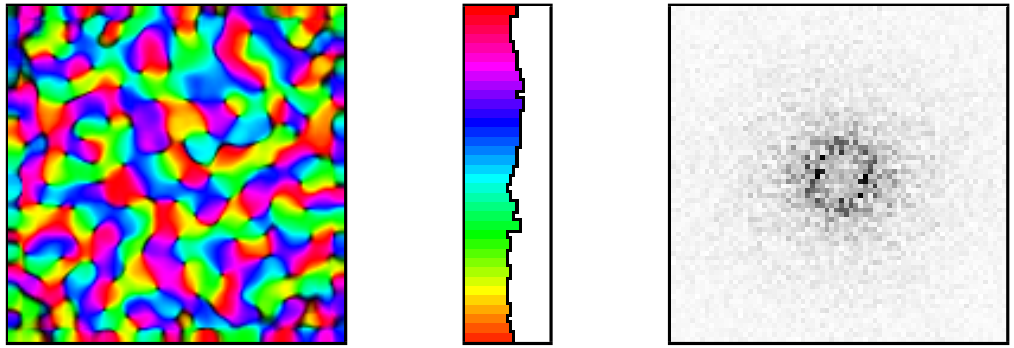

CMVC figure 5.13

OR Map: +/- Gaussian

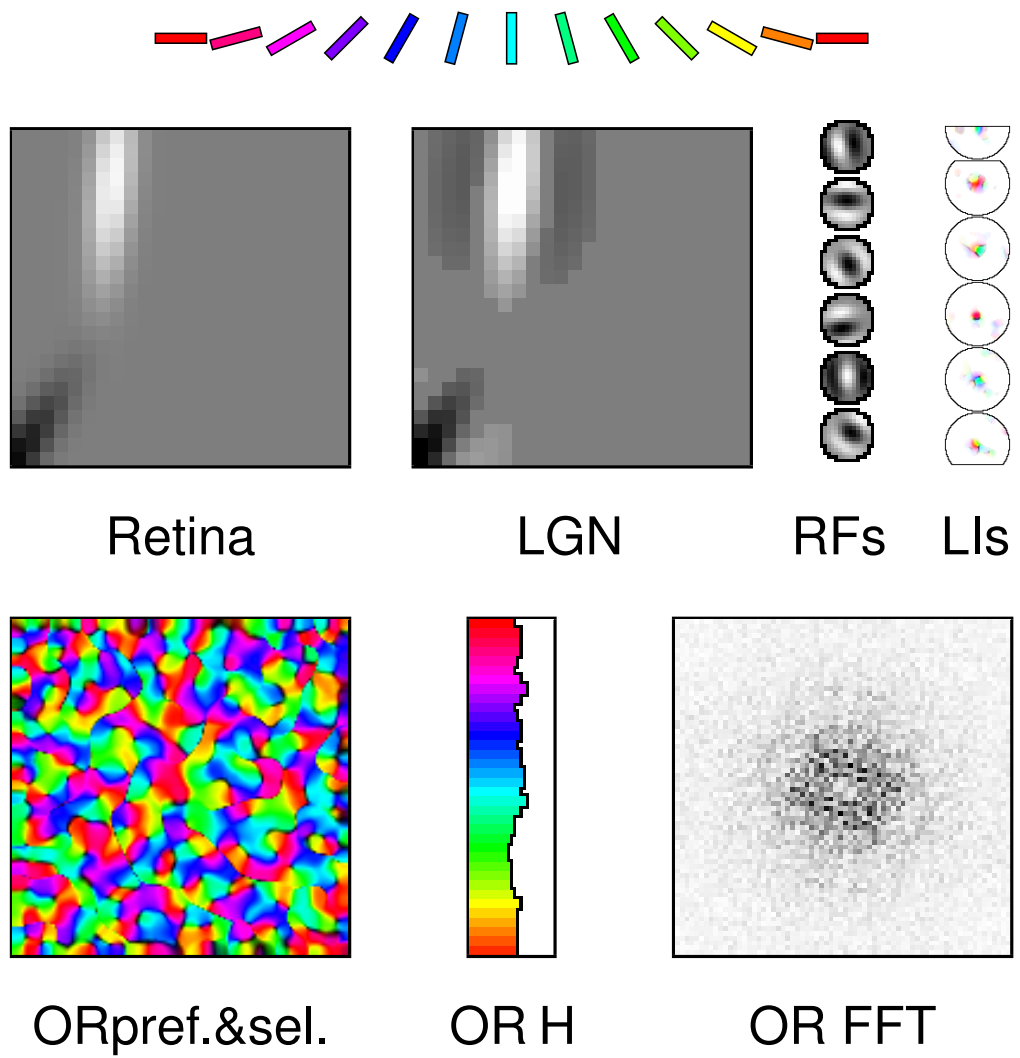

CMVC figure 5.13

White or black line

RFs

OR Map: Retinal wave model

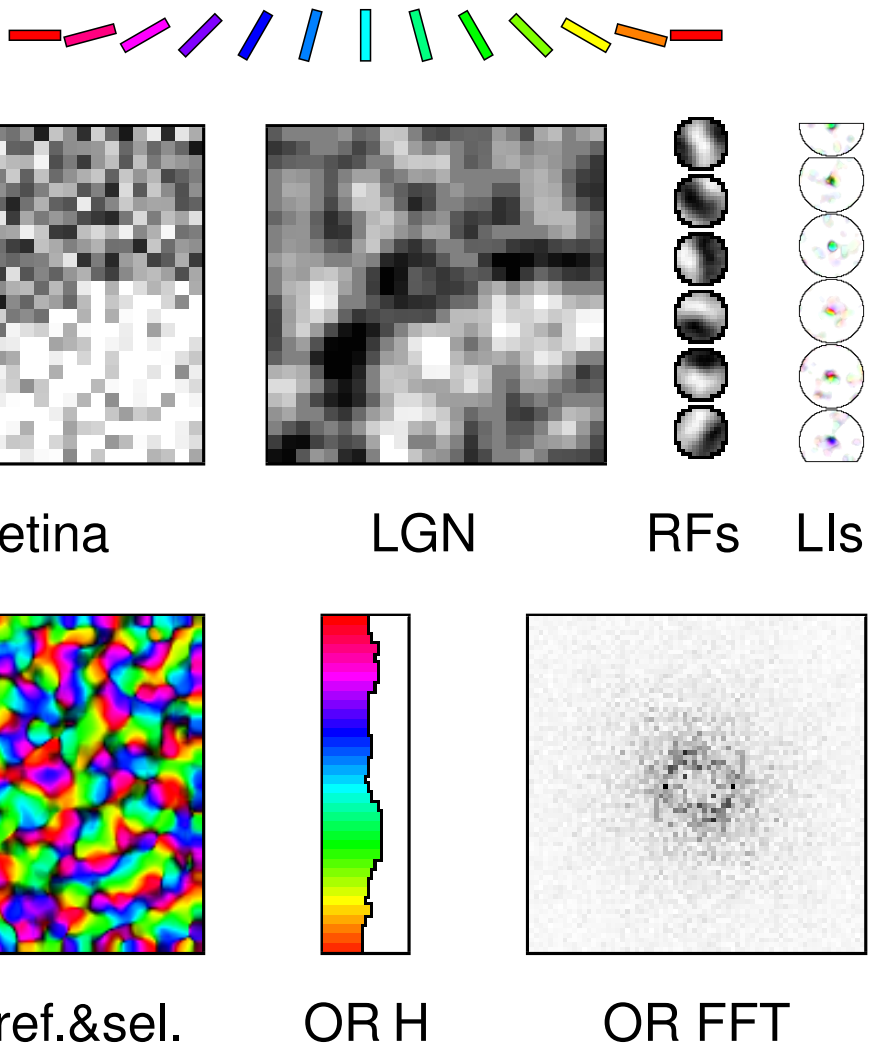

CMVC figure 5.13

Some line, mostly edge RFs

OR Map: Smooth disks

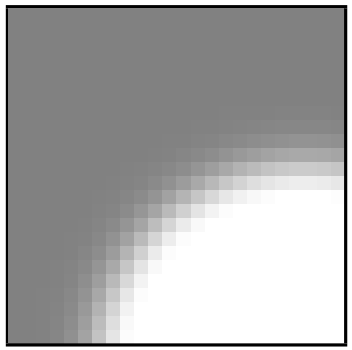

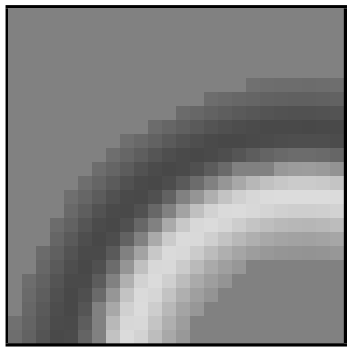

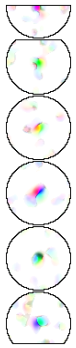

Retina LGN RFs LIs

All edge RFs

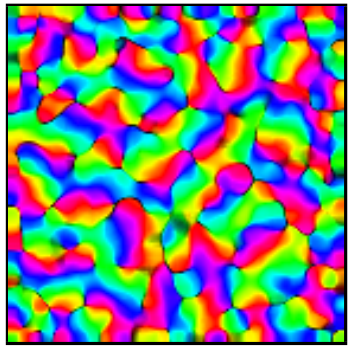

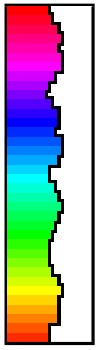

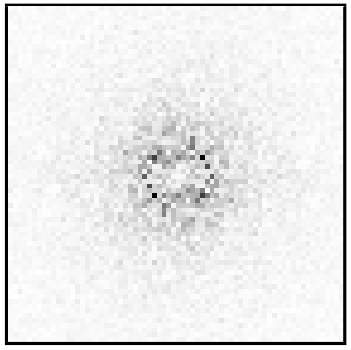

ORpref.&sel. OR H OR FFT

CMVC figure 5.13

OR Map: Natural images

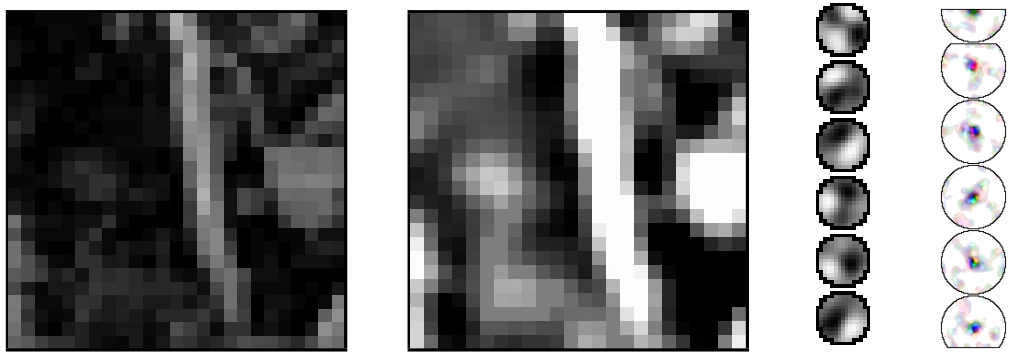

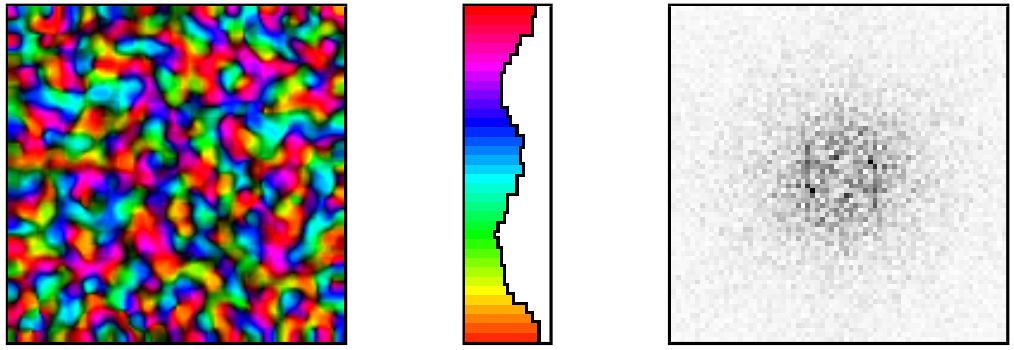

CMVC figure 5.13

All types of RFs

Longer range lateral weights

Histogram: horizontal, vertical bias

OR Map: Uniform noise

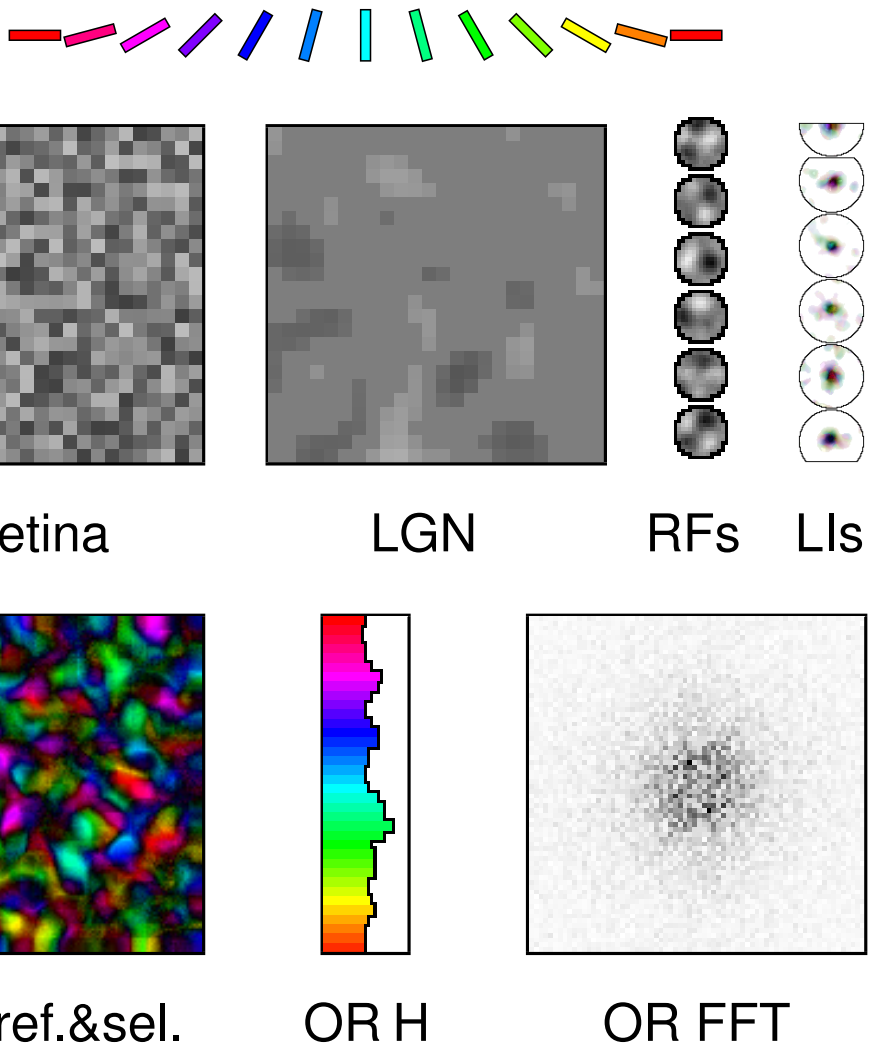

CMVC figure 5.13

Relatively unselective RFs

Modeling pre/post-natal phases

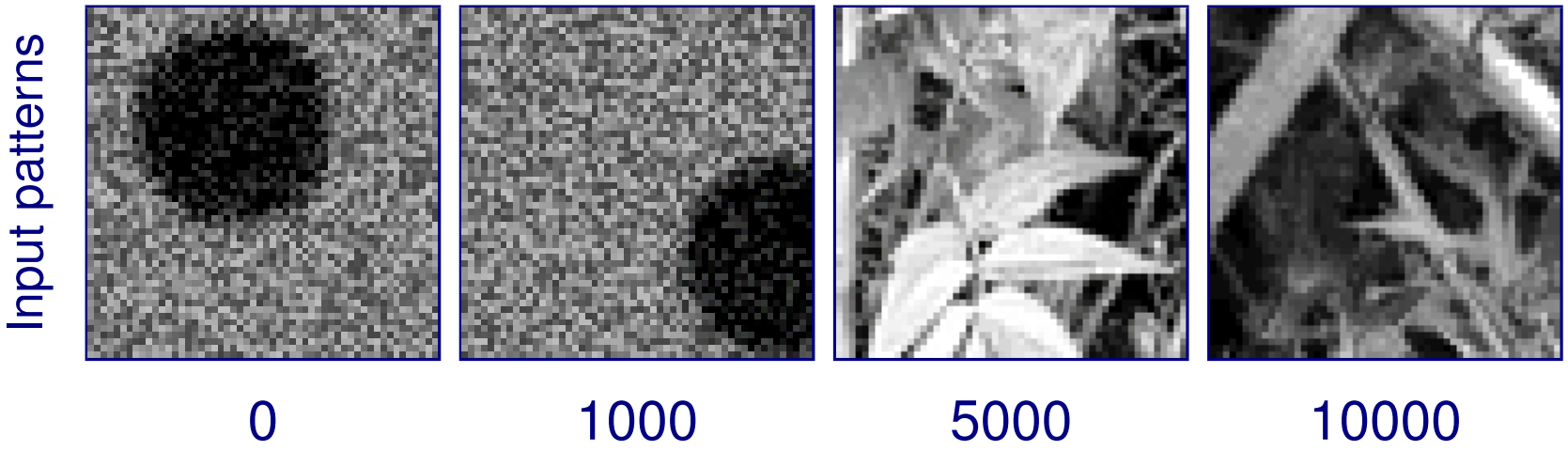

- **Prenatal:** internal activity
- **Postnatal:** natural images (Shouval et al. 1996)

Pre/post-natal V1 development

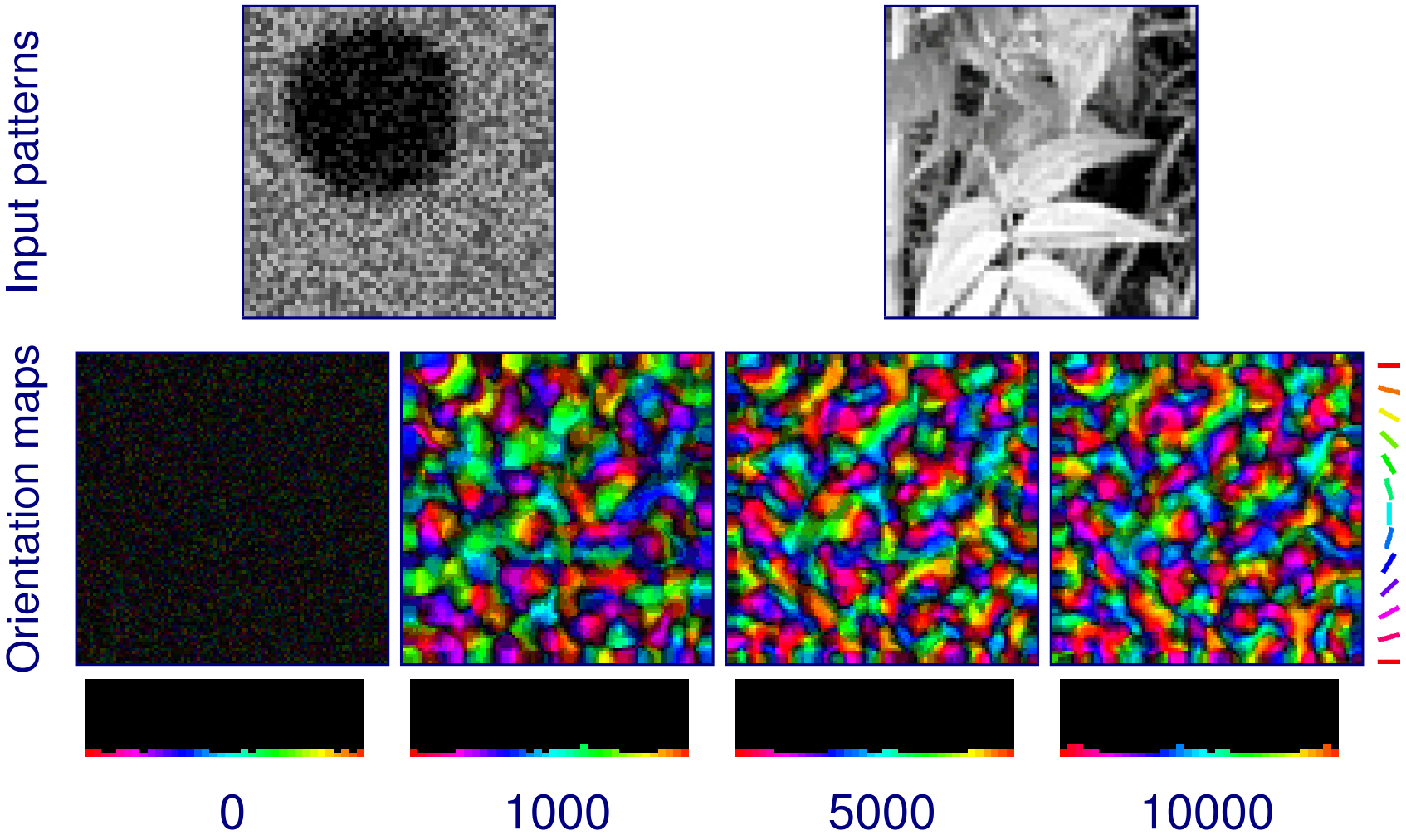

- Neonatal map smoothly becomes more selective

Statistics drive development

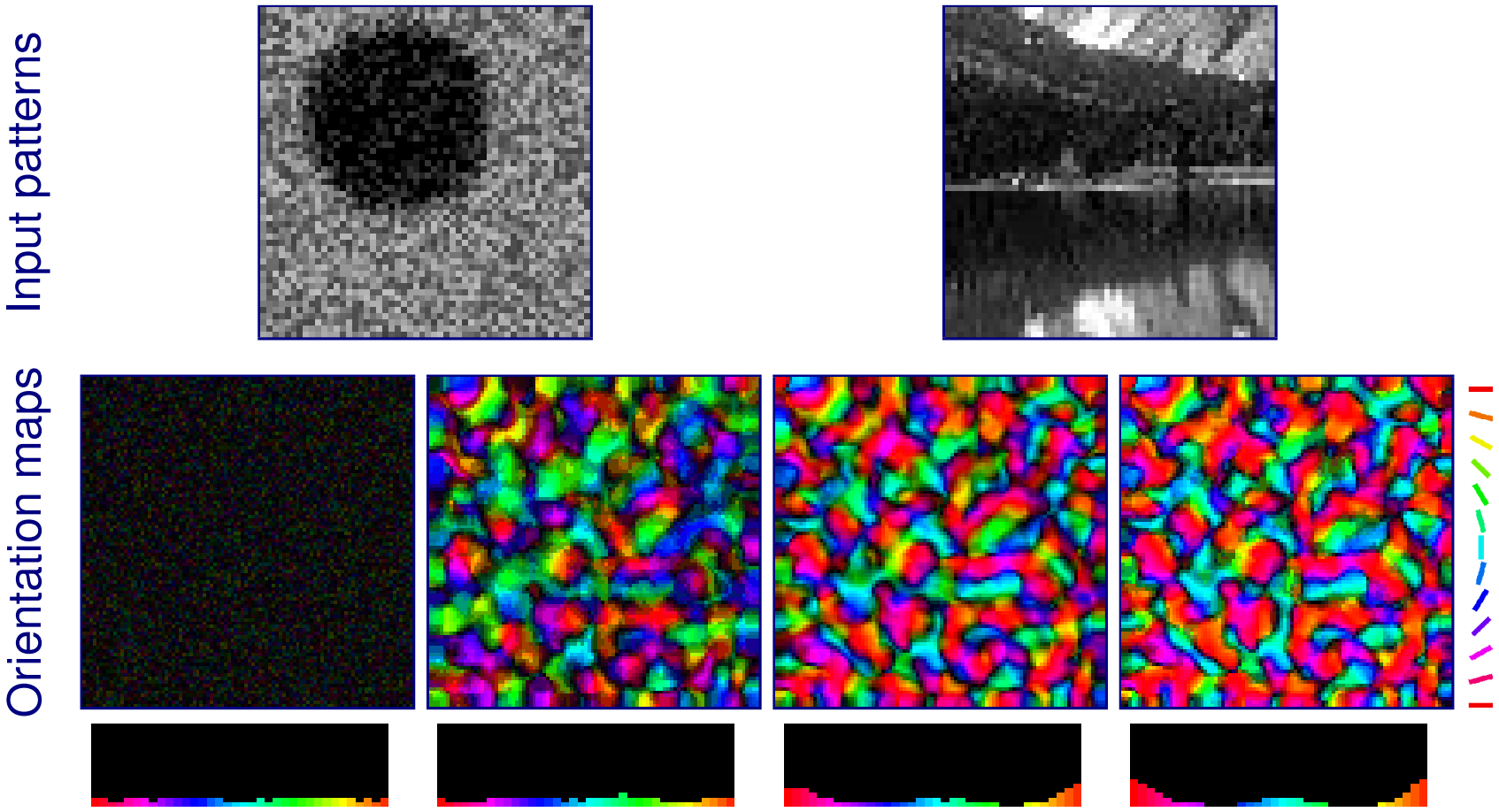

- Biased image dataset: mostly landscapes
- Smoothly changes into horizontal-dominated map

OR Histograms

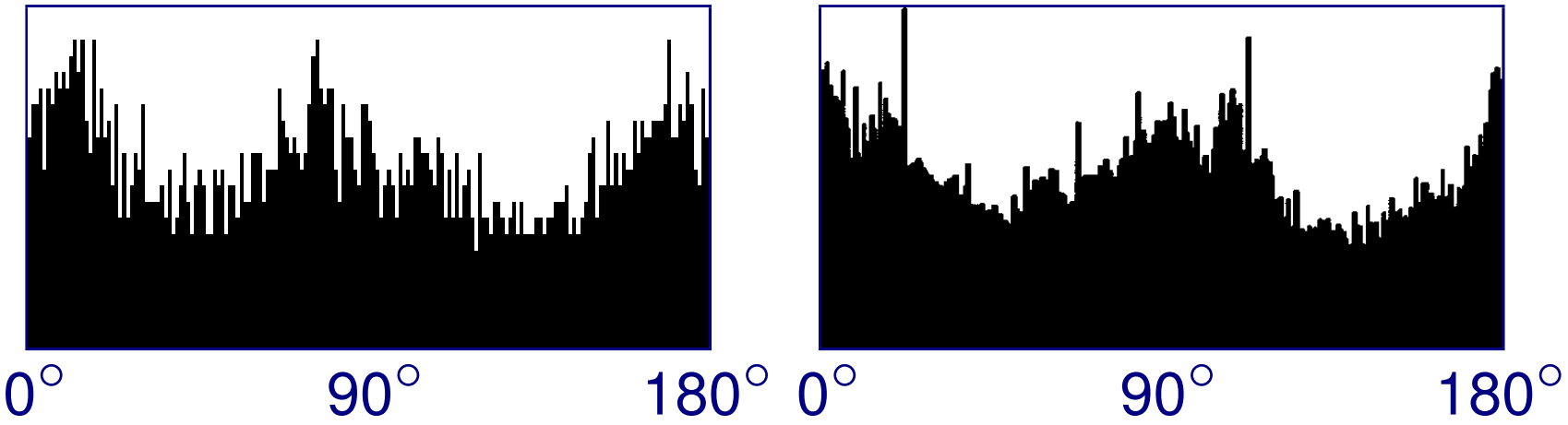

HLISSOM model

Adult ferret V1

(Coppola et al. 1998)

- After postnatal training on Shouval natural images, orientation histogram matches results from ferrets
- Model adapts to statistical structure of images

Stable development

Standard LISSOM

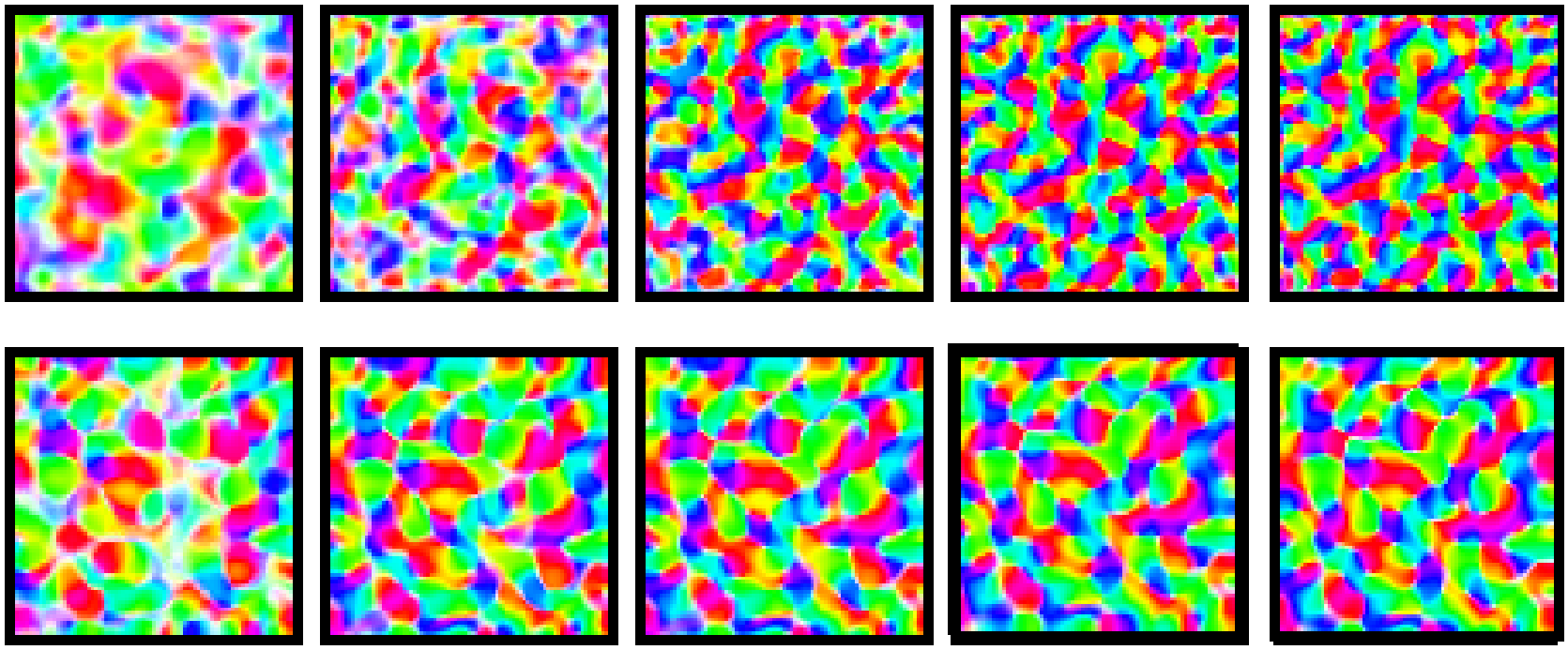

(Law 2009)

Early GCAL version (see Bednar 2012; Law et al. 2011)

If the manual thresholds of standard LISSOM are replaced with homeostatic plasticity, excitatory radius shrinking can be eliminated. Result: map shape remains stable over time.

Summary

- Development depends on features of input pattern
- Orientation maps develop with many different patterns
- Develops Gabor-type RFs with most inputs
- Breaks up image into oriented patches
- Scale response by local contrast to work for large images
- Matching biology requires prenatal, postnatal phases
- Can get more elaborate: complex cells, multiple laminae/cell types, short-range inhibition, feedback, ...

References

Bednar, J. A. (2012). Building a mechanistic model of the development and function of the primary visual cortex. *Journal of Physiology (Paris)*. In press.

Coppola, D. M., White, L. E., Fitzpatrick, D., & Purves, D. (1998). Unequal representation of cardinal and oblique contours in ferret visual cortex. *Proceedings of the National Academy of Sciences, USA*, *95* (5), 2621–2623.

Law, J. S. (2009). *Modeling the Development of Organization for Orientation Preference in Primary Visual Cortex*. Doctoral Dissertation, School of Informatics, The University of Edinburgh, Edinburgh, UK.

Law, J. S., Antolik, J., & Bednar, J. A. (2011). Mechanisms for stable and robust development of orientation maps and receptive fields. Tech. rep., School of Informatics, The University of Edinburgh. EDI-INF-RR-1404.

Miikkulainen, R., Bednar, J. A., Choe, Y., & Sirosh, J. (2005). *Computational Maps in the Visual Cortex*. Berlin: Springer.

Shouval, H. Z., Intrator, N., Law, C. C., & Cooper, L. N. (1996). Effect of binocular cortical misalignment on ocular dominance and orientation selectivity. *Neural Computation*, *8* (5), 1021–1040.